Available online at www.sciencedirect.com

ScienceDirect

Mendeleev Commun., 2021, **31**, 451–453

Mendeleev Communications

Sub- and supersolidus phase relations of formamidinium–cesium polyiodides

Artem A. Ordinartsev,[a] Andrey A. Petrov,[a] Pavel V. Dorovatovskii,[b] Roman D. Svetogorov,[b] Konstantin A. Lyssenko,[c] Eugene A. Goodilin[a,c,d] and Alexey B. Tarasov*[a,c]

[a] *Department of Materials Science, M. V. Lomonosov Moscow State University, 119991 Moscow, Russian Federation. E-mail: alexey.bor.tarasov@yandex.ru*
[b] *National Research Center 'Kurchatov Institute', 123182 Moscow, Russian Federation*
[c] *Department of Chemistry, M. V. Lomonosov Moscow State University, 119991 Moscow, Russian Federation*
[d] *Institute of General and Inorganic Chemistry, Russian Academy of Sciences, 119991 Moscow, Russian Federation*

DOI: 10.1016/j.mencom.2021.07.004

It has been demonstrated that formamidinium–cesium polyiodides are facile reagents for converting metallic lead into perovskite at temperatures of 20–90 °C. For the first time, a tentative phase diagram of the $[HC(NH_2)_2]I–I_2$ binary system was proposed, and sub- and supersolidus phase relations in the $[HC(NH_2)_2]I–CsI–I_2$ ternary system were discussed.

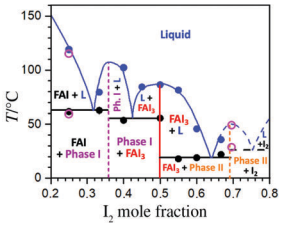

Keywords: phase diagram, polyiodides, supersolidus, formamidinium, melt processing, hybrid perovskites.

Hybrid perovskites with the general formula $APbX_3$ [A = $MeNH_3^+$ (MA), $HC(NH_2)_2^+$ (FA) and Cs^+; X = $Cl^–$, $Br^–$ and $I^–$] represent a promising class of compounds for use in photovoltaics and optoelectronics.[1–5] Recently, formamidinium-based perovskites $FA_{1–x}Cs_xPbI_3$ have attracted particular attention to their application in perovskite solar cells because of their high stability governed by entropic stabilization and the band gap of 1.55 eV, which is close to the optimal values for solar light absorption.[6–8] In particular, perovskite solar cells based on $FA_{1–x}Cs_xPbI_3$ absorbing layers demonstrated high efficiency (over 20%).[9–11]

Until now, perovskite thin films have usually been prepared by solution techniques.[12,13] However, in these methods, solution crystallization occurs through the formation of intermediate phases[14,15] that deteriorate the morphology of the film and impedes the control and reproducibility of film deposition. Recently, a new solvent-free approach based on the direct conversion of lead films into hybrid perovskite layers by liquid methylammonium and formamidinium polyiodides, known as reactive polyiodide melts (RPMs), was used to obtain $MAPbI_3$ and $(MA,FA,Cs)PbI_3$ solar cells with efficiency more than 17%.[16,17] However, there is no detailed information on the properties of the FAI–CsI–I_2 ternary system, particularly on the temperature ranges and compositions of reactive liquid phases, which is necessary to obtain promising $FA_{1–x}Cs_xPbI_3$ compositions.

From a practical point of view, the most important parameters for implementing the RPM method to obtain $FA_{1–x}Cs_xPbI_3$ perovskite films are the solidus and liquidus temperatures of the precursor $FA_{1–x}Cs_xI_n$ polyiodides. They should not exceed ~100 °C so that RPMs can be applied in a way similar to solution blade- and slot-die coating without exceeding the thermal decomposition limits of perovskites.[18,19] It is known from published data that pure cesium polyiodides have relatively high melting points. According to the phase diagram of the CsI–I_2 system,[20] the melting temperatures of the CsI_3 and CsI_4 phases are 215 and 141 °C, respectively, with a single eutectic point between CsI_4 and I_2 at T = 70 °C.

The most interesting compositions of perovskites from the point of view of their application in photovoltaics are $FA_{1–x}Cs_xPbI_3$, where $0.15 < x < 0.20$.[6,7,21] To study the system of polyiodides with mixed Cs–FA cations, we analyzed a series of $FA_{1–x}Cs_xPbI_n$ compositions with different cesium contents (x = 0.1, 0.2 and 0.3) and several iodine/cation molar ratios (n = 2, 3, 4 and 5). Visual polythermal analysis was chosen to determine the solidus and liquidus points of the FAI/CsI/I_2 ternary mixtures.[†]

During slow heating, the sample passes through the onset point of melting and finally turns into a homogeneous liquid above the liquidus (Figure 1). Figure 2 shows the onset melting and liquidus temperatures for $FA_{1–x}Cs_xI_2$, $FA_{1–x}Cs_xI_3$, $FA_{1–x}Cs_xI_4$ and $FA_{1–x}Cs_xI_5$ compositions with different cesium content. For AI_2 and AI_4 compositions, it was found that the melting temperatures and liquidus points change linearly with an increase in cesium iodide content, while for AI_3 and AI_5, the dependencies exhibited extremes. The obtained values of the solidus temperature are in good agreement with those previously reported.[17]

To understand the origin of such extremes, we carried out a powder X-ray diffraction analysis of the samples after their homogenization in the liquid state at an elevated temperature and

[†] For each measurement, the precursor mixtures were preliminarily ground in a glove box with dry air to avoid moisture ingress. After that, the powder was placed on the surface of a glass thermostatic cell, followed by encapsulation using a slide glass and Kapton tape. This configuration made it possible to observe the changes occurring in a thin layer of the mixture upon heating using an optical microscope in reflection mode. The temperature was controlled with an accuracy of about 1 °C by a thermocouple attached to the cell surface.

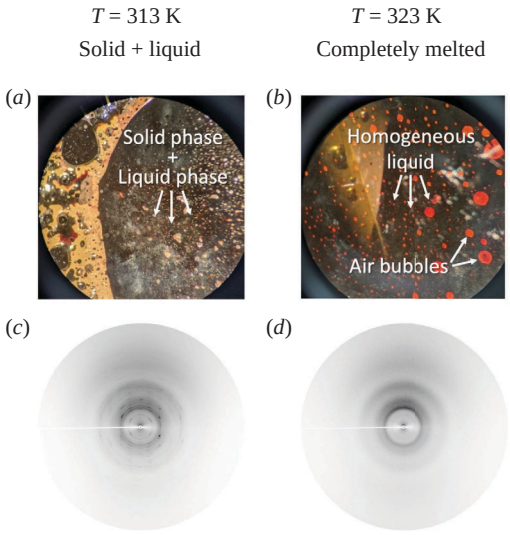

Figure 1 (*a*),(*b*) Micrographs obtained from visual polythermal analysis and (*c*),(*d*) X-ray diffraction (XRD) patterns of a mixture with $x(I_2) = 0.7$ when heated from (*a*),(*c*) 40 to (*b*),(*d*) 50 °C.

subsequent cooling to room temperature (Figure 3). Replacing the formamidinium cation in FAI_n with cesium does not shift the positions of the XRD reflections when the cesium content increases. Instead, at a high cesium content, reflections of cesium polyiodides[22,23] appear (see Figure 3). Apparently, mixed formamidinium and cesium polyiodide phases exist in the FAI–CsI–I_2 ternary system in a narrow compositional range, due to which a eutectic point and an extremum appear on the observed liquidus curves.

To better understand the character of the sub- and supersolidus relations, we performed additional experiments to study the liquidus and solidus temperatures in the FAI–I_2 binary system,

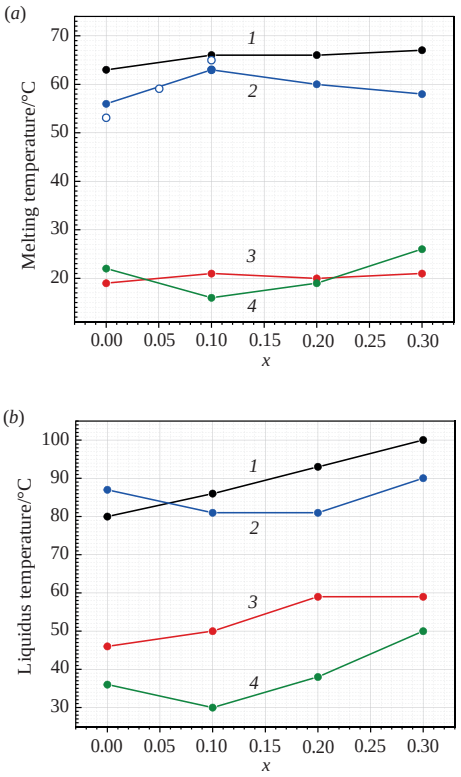

Figure 2 The dependence of (*a*) the onset melting temperature and (*b*) liquidus temperature of (*1*) $FA_{1-x}Cs_xI_2$, (*2*) $FA_{1-x}Cs_xI_3$, (*3*) $FA_{1-x}Cs_xI_4$ and (*4*) $FA_{1-x}Cs_xI_5$ mixtures on the cesium content (*x*). Each line demonstrates the same I_2/cation molar ratio. The empty circles show the melting temperatures from the cited article.[17]

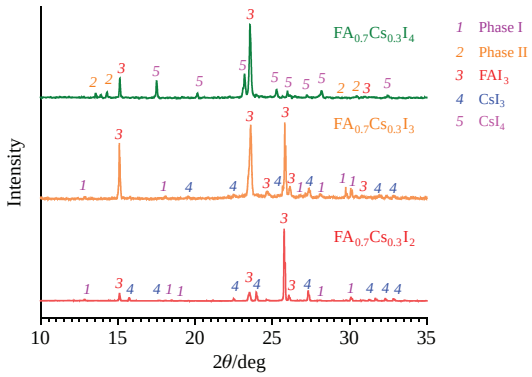

Figure 3 The XRD patterns of the $FA_{0.7}Cs_{0.3}I_2$, $FA_{0.7}Cs_{0.3}I_3$ and $FA_{0.7}Cs_{0.3}I_4$ samples after homogenization at an elevated temperature and subsequent cooling to room temperature.

using the visual polythermal analysis described above and thermal X-ray diffraction using synchrotron radiation,‡ and tentatively plotted the phase diagram (Figure 4). At an equimolar ratio of FAI and I_2, the system contains the recently reported phase FAI_3 with a melting point T_m = 87 °C.[24] The onset of melting observed at ~56 °C [Figures 2(*a*) and 4] is apparently caused by a slight deviation from stoichiometry FAI_3 towards lower iodine content and therefore reveals solidus temperature. For other compositions, according to XRD data, reflections are also present that cannot be attributed to FAI, FAI_3 or I_2, indicating the existence of lower (Phase I) and higher (Phase II) polyiodides relative to FAI_3. Based on XRD data and solidus and liquidus behavior, we assume that the composition of Phase I is close to FAI_2. Diffraction experiments at a synchrotron for a mixture with $x(I_2) = 0.7$ showed that iodine reflection occurs when the sample is cooled below the solidus temperature. Additionally, the solidus temperature was found to be higher than that of FAI_5. Based on these facts, we hypothesize that the Phase II composition may be close to $FAI_{5.5}$, similarly to the recently refined $MAI_{5.5}$.[25] Accordingly, we assume four eutectics in the FAI–I_2 system, the deepest of which is at $0.6 < x(I_2) < 0.7$ with a temperature of ~20 °C.

From a material preparation point of view, it is assumed that at least some liquid phase is present to significantly improve mass transfer and ensure efficient conversion of lead metal to perovskite

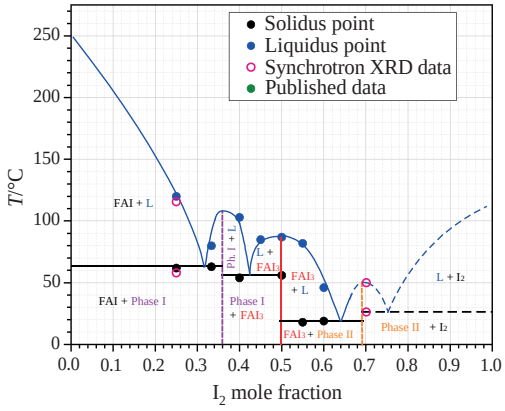

Figure 4 Tentative phase diagram of the FAI–I_2 binary system. The dashed lines show the approximate position of the area border, which needs to be clarified further. The black and blue dots represent the experimental data obtained by visual polythermal analysis, and the magenta circles are the data from the synchrotron XRD experiments.

‡ A preliminarily melted sample was placed in a capillary 200 μm in diameter, and the diffraction pattern was analyzed at a given temperature. The liquidus temperature was determined from the disappearance of the diffraction pattern, while the solidus point was considered reached when the diffraction pattern ceased to change upon cooling (see Figure 3).

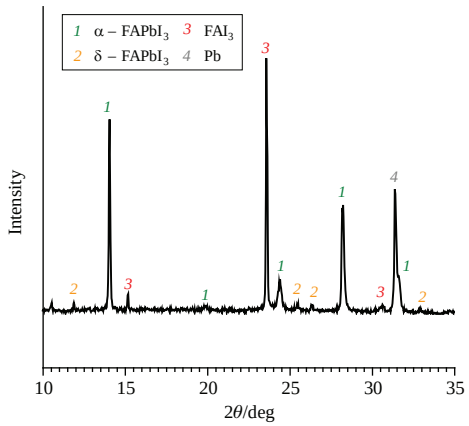

Figure 5 XRD pattern of a film obtained by converting a 600-nm lead metal film with FAI_3 at 70 °C for 30 min. The reflection at ~10.5° presumably refers to a formamidinium-excessive phase.

film over a relatively wide temperature range. According to $FAPbI_3$ stoichiometry, the left border of the composition range should be set at FAI_3. The right border should be close to $FAI_{5.5}$ since PbI_2 can be observed as the main product of lead conversion if molecular iodine (I_2) is present in equilibrium with polyiodides, as shown for the MAI–I_2 system.[16,25] Consequently, the appropriate composition range for the application of the RPM approach extends from FAI_3 to $FAI_{5.5}$ with the solidus at around 20 °C and the liquidus varying from 20 to 87 °C.

It has surprisingly been found that the solid FAI_3 phase reacts with metallic lead at an elevated temperature below its melting point. A thin film of metallic lead, deposited by vacuum evaporation on a glass substrate, was converted mainly to the α-$FAPbI_3$ phase in 30 min by attaching to another glass substrate with drop-cast FAI_3 (Figure 5), which suggests that FAI_3 will play the role of a new facile precursor for FA-based perovskites.

This work was supported by the Russian Science Foundation (project no. 18-73-10224). A.P. and E.G. thank colleagues from the Joint Research Center for Physical Methods of Research of IGIC RAS for their valuable assistance in sample analysis. K.L. acknowledges partial support by the Moscow State University Program of Development. The authors are grateful to Nikolai Belich for help in designing metallic lead conversion experiments and Sergey Fateev for help in developing a thermostatic cell and scientific advice.

References

1 Q. Lin, A. Armin, R. C. Raju Nagiri, P. L. Burn and P. Meredith, *Nat. Photonics*, 2015, **9**, 106.
2 S. De Wolf, J. Holovsky, S.-J. Moon, P. Löper, B. Niesen, M. Ledinsky, F.-J. Haug, J.-H. Yum and C. Ballif, *J. Phys. Chem. Lett.*, 2014, **5**, 1035.
3 W. Li, Z. Wang, F. Deschler, S. Gao, R. H. Friend and A. K. Cheetham, *Nat. Rev. Mater.*, 2017, **2**, 16099.
4 J. Huang, Y. Yuan, Y. Shao and Y. Yan, *Nat. Rev. Mater.*, 2017, **2**, 17042.
5 N.-G. Park, M. Grätzel, T. Miyasaka, K. Zhu and K. Emery, *Nat. Energy*, 2016, **1**, 16152.
6 C. Yi, J. Luo, S. Meloni, A. Boziki, N. Ashari-Astani, C. Grätzel, S. M. Zakeeruddin, U. Röthlisberger and M. Grätzel, *Energy Environ. Sci.*, 2016, **9**, 656.
7 J. Huang, P. Xu, J. Liu and X.-Z. You, *Small*, 2017, **13**, 1603225.
8 J. A. Schwenzer, T. Hellmann, B. A. Nejand, H. Hu, T. Abzieher, F. Schackmar, I. M. Hossain, P. Fassl, T. Mayer, W. Jaegermann, U. Lemmer and U. W. Paetzold, *ACS Appl. Mater. Interfaces*, 2021, **13**, 15292.
9 Z. Peng, Q. Wei, H. Chen, Y. Liu, F. Wang, X. Jiang, W. Liu, W. Zhou, S. Ling and Z. Ning, *Cell Rep. Phys. Sci.*, 2020, **1**, 100224.
10 Z. Wang, Q. Lin, B. Wenger, M. G. Christoforo, Y.-H. Lin, M. T. Klug, M. B. Johnston, L. M. Herz and H. J. Snaith, *Nat. Energy*, 2018, **3**, 855.
11 J. Yang, Y. Chen, W. Tang, S. Wang, Q. Ma, Y. Wu, N. Yuan, J. Ding and W.-H. Zhang, *J. Energy Chem.*, 2020, **48**, 217.
12 J. Seo, J. H. Noh and S. I. Seok, *Acc. Chem. Res.*, 2016, **49**, 562.
13 S. I. Seok, M. Grätzel and N.-G. Park, *Small*, 2018, **14**, 1704177.
14 A. A. Petrov, S. A. Fateev, V. N. Khrustalev, Y. Li, P. V. Dorovatovskii, Y. V. Zubavichus, E. A. Goodilin and A. B. Tarasov, *Chem. Mater.*, 2020, **32**, 7739.
15 R. Szostak, P. E. Marchezi, A. dos Santos Marques, J. C. da Silva, M. Serra de Holanda, M. Medeiros Soares, H. C. Nogueira Tolentino and A. F. Nogueira, *Sustainable Energy Fuels*, 2019, **3**, 2287.
16 A. A. Petrov, N. A. Belich, A. Y. Grishko, N. M. Stepanov, S. G. Dorofeev, E. G. Maksimov, A. V Shevelkov, S. M. Zakeeruddin, M. Graetzel, A. B. Tarasov and E. A. Goodilin, *Mater. Horiz.*, 2017, **4**, 625.
17 I. Turkevych, S. Kazaoui, N. A. Belich, A. Y. Grishko, S. A. Fateev, A. A. Petrov, T. Urano, S. Aramaki, S. Kosar, M. Kondo, E. A. Goodilin, M. Graetzel and A. B. Tarasov, *Nat. Nanotechnol.*, 2019, **14**, 57.
18 Z. Li, T. R. Klein, D. H. Kim, M. Yang, J. J. Berry, M. F. A. M. van Hest and K. Zhu, *Nat. Rev. Mater.*, 2018, **3**, 18017.
19 N.-G. Park and K. Zhu, *Nat. Rev. Mater.*, 2020, **5**, 333.
20 F. E. Rosztoczy and D. Cubicciotti, *J. Phys. Chem.*, 1965, **69**, 1687.
21 P. Luo, S. Zhou, Y. Zhou, W. Xia, L. Sun, J. Cheng, C. Xu and Y. Lu, *ACS Appl. Mater. Interfaces*, 2017, **9**, 42708.
22 H. A. Tasman and K. H. Boswijk, *Acta Crystallogr.*, 1955, **8**, 59.
23 E. E. Havinga, K. H. Boswijk and E. H. Wiebenga, *Acta Crystallogr.*, 1954, **7**, 487.
24 A. A. Ordinartsev, A. A. Petrov, K. A. Lyssenko, A. V. Petrov, E. A. Goodilin and A. B. Tarasov, *Acta Crystallogr., Sect. E: Crystallogr. Commun.*, 2021, **77**, 692.
25 A. A. Petrov, S. A. Fateev, Y. V Zubavichus, P. V Dorovatovskii, V. N. Khrustalev, I. A. Zvereva, A. V. Petrov, E. A. Goodilin and A. B. Tarasov, *J. Phys. Chem. Lett.*, 2019, **10**, 5776.

Received: 4th May 2021; Com. 21/6555